P-glycoprotein–actin association through ERM family proteins: a role in P-glycoprotein function in human cells of lymphoid origin

Francesca Luciani, Agnese Molinari, Francesco Lozupone, Annarica Calcabrini, Luana Lugini, Annarita Stringaro, Patrizia Puddu, Giuseppe Arancia, Maurizio Cianfriglia, and Stefano Fais

P-glycoprotein is a 170-kd glycosylated transmembrane protein, expressed in a variety of human cells and belonging to the adenosine triphosphate–binding cassette transporter family, whose membrane expression is functionally associated with the multidrug resistance phenotype. However, the mechanisms underlying the regulation of P-glycoprotein functions remain unclear. On the basis of some evidence suggesting P-glycoprotein–actin cytoskeleton interaction, this study investigated the association of P-glycoprotein with ezrin, radixin, and moesin, a class of proteins that cross-link actin filaments with plasma membrane in a human cell line of lymphoid origin and that have been shown to link other ion-pump–related proteins. To this purpose, a multidrug-resistant variant of CCRF-CEM cells (CEM-VBL100) was used as a model to investigate the following: (1) the cellular localizations of P-glycoprotein and ezrin, radixin, and moesin and their molecular associations; and (2) the effects of ezrin, radixin, and moesin antisense oligonucleotides on multidrug resistance and P-glycoprotein function. The results showed that: (1) P-glycoprotein colocalized and coimmunoprecipitated with ezrin, radixin, and moesin; and (2) treatment with antisense oligonucleotides for ezrin, radixin, and moesin restored drug susceptibility consistently with inhibition of both drug efflux and actin–P-glycoprotein association and induction of cellular redistribution of P-glycoprotein. These data suggest that P-glycoprotein association with the actin cytoskeleton through ezrin, radixin, and moesin is key in conferring to human lymphoid cells a multidrug resistance phenotype. Strategies aimed at inhibiting P-glycoprotein–actin association may be helpful in increasing the efficiency of both antitumor and antiviral therapies. (Blood. 2002;99:641-648)

© 2002 by The American Society of Hematology

Introduction

P-glycoprotein (P-gp) is a 170-kd glycosylated integral plasma membrane protein belonging to the adenosine triphosphate (ATP)-binding cassette transporter family. The multidrug resistant (MDR) phenotype is often associated with an increased expression of P-gp at the plasma membrane.[1] ATP hydrolysis provides energy to mediate the drug efflux against step concentration gradients, allowing the export of a variety of structurally and functionally unrelated compounds, including anticancer drugs such as vinca alkaloids, anthracyclines, taxoids, and other antimitotics.[2-8] P-gp is expressed in a variety of human cells, either in normal or pathologic conditions.[9-11] However, the mechanisms underlying the regulation of P-gp functions remain unclear, although numerous fluorescent (FL) dyes such as daunomycin and FL-bodipy drugs are efficiently transported, providing a convenient method in the screening of P-gp activity.[12] In in vitro cell systems, the level of P-gp expression correlates with the final concentration of the anticancer compound used for MDR variant selection.[13] Of interest, some evidence has suggested an important role of the actin cytoskeleton in P-gp–mediated multidrug resistance. In fact, the organization of actin filaments may be involved in the expression of P-gp function in MDR osteosarcoma cells,[14] and cytoskeleton alterations occur in an MDR human breast cancer cell line.[15] There is growing evidence that the actin-filament association with a variety of cellular proteins is mediated by a class of highly specialized molecules, ezrin/radixin/moesin (ERM) proteins, concentrated in actin-rich cell-surface structures.[16,17] These proteins cross-link actin filaments with the plasma membrane and are involved in determining cell polarization.[18,19] The interactions between plasma membrane and cytoskeleton play an essential role in cell signaling, membrane trafficking, and various cellular functions,[20-25] including cell–cell adhesion, cell motility, and apoptosis.[16,17,19,22-28] Notably, ion pumps, together with other membrane proteins, are mostly localized in well-established polarized sites of epithelial cells.[29,30] The polarization of these pumps may change depending on the distribution and composition of the cytoskeleton,[29] as well as on the direct or indirect association of the pump-associated proteins with the actin cytoskeleton through the ERM proteins.[31] Moreover, we have recently shown that treatment with interferon-γ (IFN-γ) induced in human monocyte-derived macrophages the translocation of P-gp to the plasma membrane, where it polarized and colocalized with ezrin,[11] suggesting P-gp interaction with the actin cytoskeleton through ERM proteins. On the basis of these data, we have focused our investigation on the P-gp–actin interactions through ERM proteins and the role of these interactions in P-gp–mediated multidrug resistance in human cells of lymphoid origin. For this study, we used parental CCRF-CEM cells and its MDR variant P-gp–expressing CEM-VBL100 as a model to investigate the following: (1) the level of polarization; (2)

the cellular expression, distribution, and the molecular association of P-gp with ERM proteins; and (3) the effects of ERM antisense oligonucleotides on susceptibility to drug-mediated cytotoxicity, drug efflux, and P-gp subcellular localization, as well as its association with actin. The results clearly showed that: (1) parental and CEM-VBL100 cells both expressed high levels of ezrin, radixin, and moesin; (2) P-gp polarized, colocalized, and coimmunoprecipitated with ERM proteins in CEM-VBL100 cells; and (3) treatment with ERM antisense oligonucleotides de novo induced drug susceptibility, inhibition of the drug efflux system (resulting in an increase in intracellular drug retention), and P-gp molecule redistribution and its dissociation from actin. Together these results suggest that actin–P-gp association is a key mechanism in determining MDR phenotype at the cellular level.

Materials and methods

Cells and chemicals

The MDR variant (CEM-VBL100) of CCRF-CEM (CEM) cells was obtained by exposing the parental drug-sensitive human T-lymphoblastoma cell line to increasing sublethal concentrations of vinblastine sulfate (VBL) up to 100 ng/mL (Eli Lilly, Paris, France).[13] All the cells used in this study were cultured in RPMI 1640 medium enriched with 10% fetal bovine serum and antibiotics (basic medium, BM) in a humidified 5% CO_2 and 95% air atmosphere. P-gp drug efflux was measured by the dye compound VBL-bodipy (50 ng/mL; Molecular Probes, Eugene, OR). The cytotoxicity assay was performed by treating cells with VBL (50 ng/mL). As a control, P-gp activity of the CEM-VBL100 cells was blocked using a 1-hour pretreatment with 10 μg/mL verapamil (VRP; Basf-Knoll, Milan, Italy).

Immunocytochemistry

CEM cells were spun onto glass slides (Shandon, United Kingdom) or attached to poly-L-lysine–covered glass chamber slides (Labtek, IL), fixed, and stained by immunocytochemistry with monoclonal antibodies (mAbs) to MDR1 (clone MM4.17, directed to an external P-gp domain),[32] actin (Chemicon, CA), ezrin (Biogenesis, United Kingdom), and moesin (Transduction Laboratories, KY), or polyclonal antibody (pAb) to radixin (Santa Cruz, CA). Staining was performed by the alkaline phosphatase–anti-alkaline phosphatase (APAAP) method (Dako, Denmark) or the peroxidase-antiperoxidase (PAP) method (Dako) with counterstaining with Mayer hemalum (BDH) (Milan, Italy).[33]

Reverse transcriptase–polymerase chain reaction analysis

Cells were pelleted and washed in cold phosphate-buffered saline (PBS). Total RNA (1 μg), obtained using the RNA-zol method (Biotech Italia, Milan, Italy), was reverse transcribed at 37°C for 1 hour in a 20-μL reaction containing 50 mM Tris-HCl, 40 mM KCl, 6 mM $MgCl_2$, 10 mM dithioerythritol (pH 8.3), and Moloney murine leukemia virus reverse transcriptase (Roche, Germany). The cDNA product was amplified in a 20-μL reaction containing 10 mM Tris-HCl (pH 8.3); 50 mM KCl; 1.5 mM $MgCl_2$; 0.001% (wt/vol) gelatin; 0.2 mM each of dATP, dGTP, dCTP, and dTTP; 5 ng/mL each of the gene-specific upstream and downstream primers; and 0.5 U Taq polymerase (Perkin Elmer, NY). The sequences of the primers used are: ezrin, 5′-CACGCTTGTCTTTAGTGCTTC-3′ and 5′-ACTCAGACTTTACAGGCATTTTCC-3′ (236-bp product); radixin, 5′-GCTAGGTGTTGATGCTTTGG-3′ and 5′-GACGTTCCATTAGCTCT-TCC-3′ (420-bp product); moesin, 5′-TCCTATGGGAGTCAAGTGTGG-3′ and 5′-AGGTCCTGTTCTCATTCCTAGACC-3′ (123-bp product); and P-gp as described previously.[34,35] Reduced glyceraldehyde 3-phosphate dehydrogenase (GAPDH) reverse transcriptase–polymerase chain reaction (RT-PCR) (primers 5′-CCATGGAGAAGGCTGGGG-3′ and 5′-CAAAGT-TGTCATGGATGACC-3′; 195-bp product) was run in parallel to normalize the levels of human RNA in all the samples. The samples were amplified for 30 to 35 cycles under the following conditions: ezrin, radixin, and moesin,

40 seconds at 94°C, 40 seconds at 62°C, and 40 seconds at 72°C; and P-gp and GAPDH, 30 seconds at 94°C, 1 second at 55°C, and 2 seconds at 94°C. A negative control lacking template was included in each experiment. The products were analyzed on a 1.5% agarose gel.

Western blot analysis

Subcellular membrane/cytoskeleton fractions from CEM cells were prepared as described previously.[36] Briefly, cells were pelleted, washed in PBS, resuspended in hypotonic solution (10 mM HEPES, pH 6.9, 10 mM KCl, 3 μL/mL aprotinin, 0.1 mM phenylmethylsulfonyl fluoride [PMSF]), and incubated on ice for 15 to 20 minutes. Cells were disrupted by dounce homogenization (20 strokes). Nuclei were pelleted at 3200 rpm for 3 minutes at 4°C and removed. The supernatant from pelleted nuclei was further centrifuged at 35 000 rpm for 20 minutes at 4°C. The supernatant (cytosol) was separated and the pellet (cytoskeletal plus membrane fraction) was further resuspended in NTENT buffer (150 mM NaCl, 10 mM Tris-HCl, pH 7.2, 1 mM EDTA, 3 μL/mL aprotinin, 0.1 mM PMSF, 1% Triton X-100).[36] Subcellular fractions were resuspended in sodium dodecyl sulfate (SDS) sample buffer, denatured by boiling, and separated on 5% or 8% SDS-polyacrylamide gel electrophoresis (PAGE). Proteins were then transferred to Protran BA85 nitrocellulose membrane (Schleicher and Schuell, Dassel, Germany) and blocked in 5% milk overnight. P-gp, ezrin, moesin, and actin were detected with anti–P-gp (JSB-1; Chemicon), anti-ezrin (Transduction Laboratories, KY), anti-moesin (Transduction Laboratories), and anti-actin (Chemicon) mAbs, respectively, and visualized with peroxidase-conjugated anti-mouse Ig (Amersham Pharmacia Biotech, Milan, Italy), followed by enhanced chemiluminescence (ECL, SuperSignal Substrate; Pierce, IL). Radixin was detected with an anti-radixin goat pAb (which recognizes radixin as well as moesin; Santa Cruz, CA) and visualized with peroxidase-conjugated anti-goat Ig (Jackson ImmunoResearch Laboratories, PA) followed by SuperSignal Substrate ECL (Pierce).

Coimmunoprecipitation analysis

Cytoskeletal/membrane fractions obtained from CCRF-CEM and CEM-VBL100 cells were precleared with protein A+G-sepharose 4B Fast Flow (Sigma, St Louis, MO) for 1 hour at 4°C. Actin, ezrin, moesin, radixin, and CD4 proteins were immunoprecipitated from precleared lysate with anti-actin (Chemicon), anti-ezrin (clone 3C12; Sigma), anti-moesin (Santa Cruz), anti-radixin (Santa Cruz), and anti-CD4 (Santa Cruz) antibodies, respectively, overnight at 4°C in the presence of protein A+G-sepharose (4B Fast Flow; Sigma). Alternatively, P-gp was immunoprecipitated as described above for ERM proteins, using an anti–P-gp mAb (clone JSB-1; Chemicon). Immunoprecipitated beads were washed 4 times in NTENT buffer, resuspended in SDS sample buffer, and resolved in 8% SDS-PAGE. Immunoprecipitated proteins were transferred to Protran BA85 nitrocellulose membrane (Schleicher and Schuell) and analyzed by Western blotting with anti-actin (Chemicon), anti-ezrin (Transduction Laboratories), anti-moesin (Transduction Laboratories), anti-radixin (Santa Cruz), anti-CD4 (Novocastra, Newcastle-upon-Tyne, United Kingdom), or anti-MDR1 (clone JSB1; Chemicon) mAb, as appropriate. The immunoblotting for actin and CD4 on actin and CD4 immunoprecipitates, respectively, was performed in nonreducing conditions, resuspending the immunoprecipitates before SDS-PAGE separation in Laemmli buffer not supplemented with β-mercaptoethanol[37] to avoid the usual migration of immunoglobulin heavy chains close to the actin and CD4 molecular weights, as described previously.[27]

Scanning electron microscopy

For immunolabeling observations with back-scattered electrons, after the deposition on poly-L-lysine–pretreated glass coverslips, the cells were incubated at 37°C for 30 minutes with an anti–P-gp mAb (MRK16; Kamiya Biomedical, WA) diluted in phosphate buffer (0.15 M NaCl, 0.05 M Na_2HPO_4, 0.05 M NaH_2PO_4), containing 0.5% bovine serum albumin (BSA) and 0.05% Tween 20. Negative controls were incubated with irrelevant isotype-matched mAb. After 3 washes with the phosphate buffer,

the cells were incubated with anti-mouse IgG-gold conjugate (average diameter of the gold particles, 10 nm; Sigma) diluted in phosphate buffer at room temperature for 30 minutes, rinsed twice in the same buffer, and fixed at room temperature for 20 minutes with 2.5% glutaraldehyde containing 2% sucrose. After repeated washes in distilled water, silver enhancement (British Biocell International, United Kingdom) was performed for 10 minutes at 19°C. Finally, the samples were dehydrated on an ethanol gradient, critical point dried in CO_2, carbon coated by sputtering, and examined with a Cambridge Stereoscan 360 scanning electron microscope (Cambridge Instruments, Cambridge, United Kingdom). Observations with secondary electrons were used as a control of cell morphology.

Antisense oligonucleotides

Two antisense phosphorothioate oligonucleotides (S-modified) (PONs) complementary to the corresponding positions 1 to 15 of the human ezrin, radixin, and moesin coding regions were used. The chosen sequence was 5′-TACGGCTTTGGTTAG-3′ for the ezrin/radixin antisense (these proteins share 100% homology in this region) and 5′-TACGGGTTTT-GCTAG-3′ for the moesin antisense (Amersham, Freiburg, Germany). Each PON was resuspended in serum-free medium and added to the culture medium every 12 hours at the final concentration of 20 μM for 60 to 72 hours. Every 24 hours, CEM cells were washed and resuspended in fresh medium supplemented with 20 μM of each PON. The same region sense PONs pretreatment and untreatment were used as controls.

P-gp function assays in ERM PON-treated cells

Cell cytotoxicity. Untreated CEM-VBL100 cells and cells pretreated with sense or antisense PONs were pelleted, resuspended in BM, and seeded in a 96-well microplate at 5×10^5 cells/mL. To evaluate the activity of P-gp, we treated the cells with 50 ng/mL VBL, 10 μg/mL VRP, or both (VRP was added 1 hour before VBL). Control experiments were performed by replicating culture conditions in the absence of drugs. After an overnight incubation, the microplate was centrifuged, the supernatant was removed, and the cells were resuspended in Hanks balanced salt solution (Gibco Laboratories, NY). Thus, the live/dead viability/cytotoxicity test was performed, following the manufacturer's instructions (Molecular Probes), calculating the percentage of dead cells after each treatment.

Efflux and drug retention. Untreated or treated CEM-VBL100 cells were washed twice with fresh medium and incubated with 50 ng/mL VBL-Bodipy[38] for 15 minutes at 37°C. The samples were then centrifuged to remove the drug, washed with cold RPMI medium, and incubated in BM at 37°C for 30 minutes to 2 hours. At the end of efflux times, cells were washed twice with cold PBS and immediately analyzed with the flow cytometer. As a positive control for P-gp activity inhibition, untreated CEM-VBL100 cells were incubated with VRP during the efflux time. The percentage of drug retention was calculated as the ratio between mean fluorescence channel (MFC) of each sample at the end of the efflux time and the MFC detected at the end of drug treatment, times 100.

Laser scanning confocal microscopy

To detect P-gp expression, we attached the cells to polylysine-coated coverslips and fixed them with freshly prepared 4% formaldehyde in PBS for 10 minutes at room temperature. After washing in the same buffer, supplemented with 0.5% BSA (BSA-PBS), cells were incubated with MRK16 mAb (IgG2a, 25 μg/mL; Kamiya Biomedical) for 30 minutes at room temperature. After washing with BSA-PBS, samples were incubated with goat anti-mouse IgG fluorescein-linked antibody (Sigma, St Louis, MO) for 30 minutes at room temperature. Negative controls were obtained by incubating the samples with IgG2a isotypic globulins (Sigma). For double labeling of P-gp and ERM proteins, unfixed cells were first labeled for P-gp as described above at 4°C. After several washings, cells were fixed and permeabilized with cold methanol for 10 minutes and then incubated with goat anti-radixin, anti-moesin, or anti-ezrin (Santa Cruz) for 30 minutes at room temperature. After washing in BSA-PBS, samples were incubated with rhodamine-linked rabbit anti-goat IgG (Sigma) for 30 minutes at room temperature. Incubations with normal goat Ig (Sigma)

were used as negative controls. The analysis of the intracellular distribution of antitumor drug was performed on live cells, treated as described in the flow cytometry P-gp function assays section and mounted on glass microscope slides. To avoid cell damage, we made the image acquisitions quickly on several cells present on different slides for each sample, capturing signals from one field per slide. The observations of both living and fixed cells were made using a Leica TCS 4D laser scanning confocal microscope (Leica Microsystems, Mannheim, Germany) equipped with an Ar/Kr laser. The excitation and emission wavelengths used were 488 nm for fluorescein and VBL bodipy[9] and 568 nm for rhodamine. Fluorescence emissions were collected after passage through 510-nm and 590-nm long-pass filters for fluorescein/VBL bodipy and rhodamine, respectively. Acquisition parameters were as follows: objective, 40.0/1.0 oil; pinhole size, 113; x,y pixel size, 0.13 μm; z pixel size, 0.58 μm; and step size, 0.58 μm. Double-labeled samples were analyzed by the Multicolor Program (Leica), which allows the elimination of channel cross-talk.

Results

P-gp–ERM cellular distribution in CEM-VBL100 cells

As expected, CEM-VBL100 cells expressed high levels of P-gp at both the mRNA (Figure 1A) and protein levels (Figure 1B), whereas parental CCRF-CEM cells did not. In contrast, parental and CEM-VBL100 cells expressed equal levels of both ezrin and moesin, as assessed by both RT-PCR (Figure 1C) and Western blot
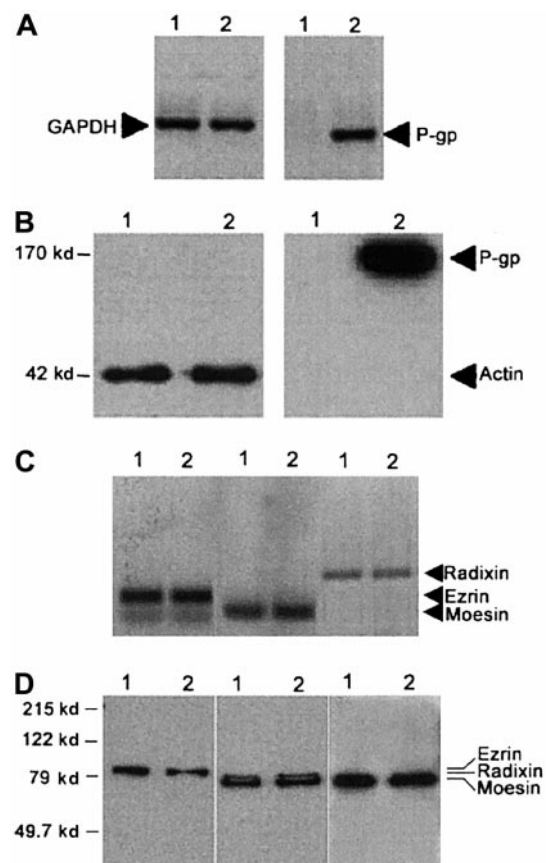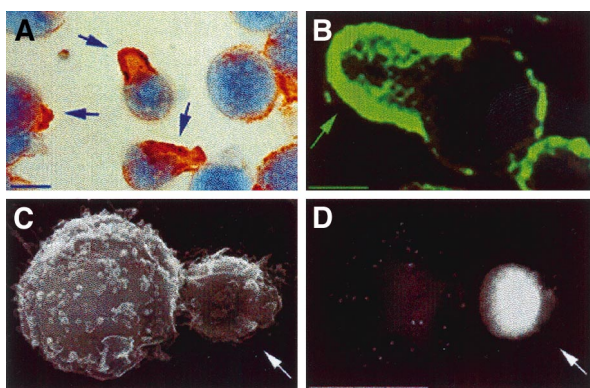

Figure 1. P-gp expression by CEM-VBL100 cells. (A) RT-PCR and (B) Western blot analyses for P-gp expression on CCRF-CEM (1) and CEM-VBL100 (2) cells. P-gp is expressed on the CEM-VBL100 cell line, derived from CEM cells by selection in medium containing 100 ng/mL VBL, and is undetectable in the parental CEM cell line at both the mRNA (A) and protein levels (B). (C) RT-PCR and (D) Western blot analysis for ERM expression on CCRF-CEM[1] and CEM-VBL100[2] cells. Both cell lines expressed comparable levels of ezrin, radixin, and moesin (C,D; arrows). GAPDH (A) and actin (B) levels in the relative lysates are shown.
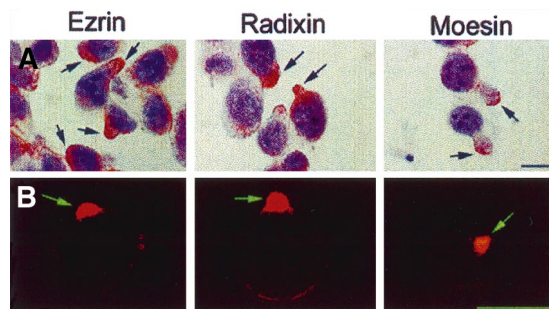
analysis (Figure 1D). Moreover, both parental and CEM-VBL100 cells, unlike other CEM cell clones and human primary lympho-cytes,[27,39] expressed detectable and comparable levels of radixin (Figure 1C,D). The MDR cells continuously underwent giant uropod and pseudopod formation during culture, and up to 90% of CEM-VBL100 cells showed P-gp polarization on uropods or pseudopods, as assessed by immunocytochemistry, immunofluores-cence, and immuno–scanning electron microscopy (SEM) (Figure 2), suggesting a possible linkage to the actin cytoskeleton. Thus, we preliminarily assessed in CEM-VBL100 cells the expression and cellular distribution of ERM. The results showed that ERM were fully expressed and polarized in this cell line, as assessed by both immunocytochemistry and immunofluorescence (Figure 3). This set of results strongly suggested colocalization and association of P-gp and ERM proteins in CEM-VBL100 cells. Thus, we per-formed a series of experiments aimed to evaluate both colocaliza-tion and molecular association between P-gp and ERM.

P-gp–ERM colocalization and coimmunoprecipitation in CEM-VBL100 cells

First, we evaluated the possible colocalization of P-gp with ERM proteins in the uropods of CEM-VBL100 cells. Laser scanning confocal microscopy (LSCM) analysis showed a clear colocaliza-tion of P-gp with ERM proteins in these cells (Figure 4A,B). Figure 4A shows CEM-VBL100 cells double-labeled for P-gp and ezrin or radixin or moesin. We further analyzed this phenomenon in optical sections of a defined region of P-gp–ERM colocalization (Figure 4B). The analysis was performed on each P-gp double staining with ezrin or radixin or moesin. The results clearly showed that P-gp colocalized with all the ERM proteins in the tip of CEM-VBL100 cell uropods. Figure 4B shows 6 magnified representative sections of the P-gp–moesin colocalization in the squared region in Figure 4A. A significant moesin–P-gp colocalization was detectable in the white areas of highly polarized regions. Figure 4B shows the most internal (upper left) to the most external (lower right) sections of the uropod double stained for moesin (red) and P-gp (green). The intermediate sections, corresponding to the juxta-membrane re-gion, clearly showed a wide overlapping (white) of the moesin–P-gp staining. These results indicate that, similar to other ERM–membrane protein colocalization,[27] the specific sites of the ERM–P-gp colocalization were in the juxta-membrane region of CEM-VBL100 cells. Notably, the polarized distribution of a protein and its colocalization with ERM proteins are the first and

most important features suggesting a molecular association with the actin cytoskeleton.[16,24,26-28] Thus, we performed coimmunopre-cipitation experiments to assess the level of P-gp association with both actin and ERM proteins in cytoskeletal/membrane subcellular fractions of CEM-VBL100 cells, as compared with those of parental CEM cells. P-gp was detectable in immunoprecipitates of actin, ezrin, radixin, and moesin obtained from CEM-VBL100 cell lysates (Figure 5A). These data were confirmed by reciprocal coimmunoprecipitation experiments in which ezrin, radixin, and moesin were clearly detectable in P-gp immunoprecipitates from CEM-VBL100 cell lysates (Figure 5B). This set of experiments suggested that P-gp could be associated with actin directly or indirectly through ERM proteins and that this association could have an important role in the MDR activity related to P-gp.

Figure 3. Distribution of ERM proteins on CEM-VBL100 cells. Immunocytochem-istry (APAAP, counterstaining with Mayer hemalum) (A) and immunofluorescence (B) analyses in CEM-VBL100 cells for ezrin (left panels), radixin (central panels), and moesin (right panels). Note the extreme level of polarization of all the proteins on pseudopods or uropods of CEM-VBL100 cells, independent of the detection method used. Bar = 5 μm.
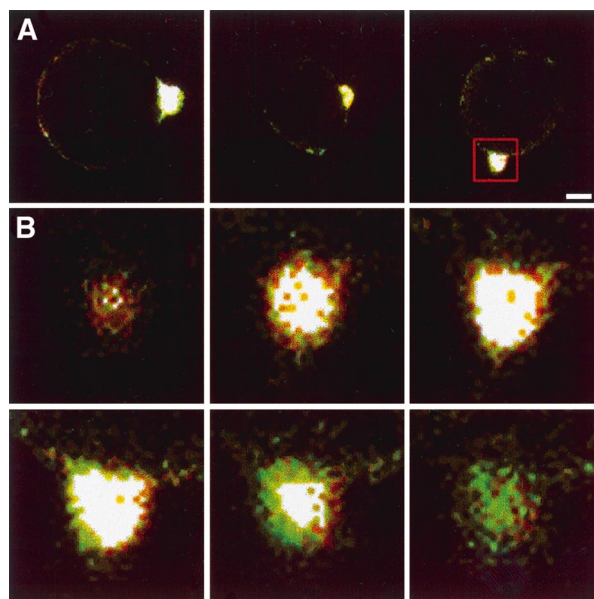

Figure 2. Distribution of P-gp on CEM-VBL100 cells. Control CEM-VBL100 cells presented uropoidal formations (arrow) on their surfaces (C, left panel). P-gp distribution on CEM-VBL100 cells appeared clearly polarized on these structures. The arrows point to the sites of P-gp polarization in immunocytochemistry (PAP, counterstaining with Mayer hemalum) (A), immunofluorescence (B), and immuno-SEM (C) analyses. Bar = 5 μm.

Figure 4. P-gp colocalization with ERM proteins. (A) Double-staining immunofluo-rescence and LSCM analysis of P-gp colocalization with ezrin (left panel), radixin (central panel), and moesin (right panel). White color is the overlapping of green (P-gp) and red (ERM) signals. Bar = 1 μm. (B) A sequence of 6 optical sections obtained by the confocal analysis of a CEM-VBL100 cell stained for P-gp (green) and moesin (red) in the area of polarization squared in panel A (right panel). The most internal (upper left) to the most external (lower right) sections of the uropod double stained for moesin (red) and P-gp (green) are shown. The intermediate sections, corresponding to the juxta-membrane region, clearly showed a wide overlapping (white) of the moesin/P-gp staining.
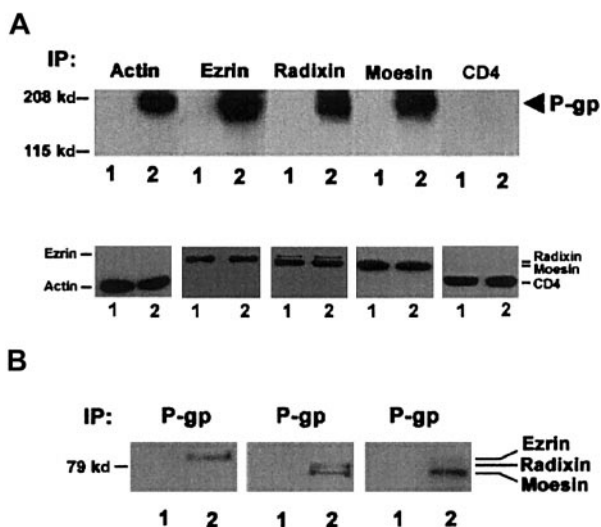
Figure 5. P-gp association with ERM proteins. (A) Upper panel: Western blotting for P-gp (arrow) in actin, ezrin, radixin, and moesin immunoprecipitates (IP) from the cytoskeletal/membrane fraction of CCRF-CEM (1) and CEM-VBL100 (2) cells. P-gp is clearly detectable in each ezrin, radixin, moesin, and actin immunoprecipitate only from CEM-VBL100 cells. Western blotting for P-gp in a CD4 immunoprecipitate from the cytoskeletal/membrane fraction of the same cell types (CD4) was included as a negative control for P-gp coimmunoprecipitation. Lower panel: Western blotting for actin, ezrin, radixin, moesin, and CD4 in actin, ezrin, radixin, moesin, and CD4 immunoprecipitates, respectively, from the cytoskeletal/membrane fraction of CCRF-CEM (1) and CEM-VBL100 (2) cells. To avoid overlapping with Ig heavy chains, actin and CD4 immunoprecipitates were separated by SDS-PAGE in nonreducing conditions (see "Materials and methods"), followed by blotting with the anti-actin or the anti CD4 mAb, respectively. The figure shows successful immunoprecipitation of each tested protein. (B) Western blotting for ezrin, radixin, and moesin in P-gp immunoprecipitates from the cytoskeletal/membrane fraction of CCRF-CEM (1) and CEM-VBL100 (2) cells. Each ERM protein is clearly detectable in P-gp immunoprecipitates only from CEM-VBL100 cell protein extracts.

Role of P-gp–ERM–actin association in multidrug resistance

We performed experiments aimed at evaluating the specific role of ERM proteins in P-gp–mediated multidrug resistance. In these experiments, we treated CEM-VBL100 cells with antisense PONs complementary to the first 15 nucleotides of the coding region of ezrin/radixin (these proteins display 100% homology in this region) and moesin. We first evaluated the effects of 60 to 72 hours of PON treatment on both ERM protein expression and viability of the cells. The results clearly showed that the 60-hour treatment with the antisense PONs markedly inhibited the expression of ERM proteins in CEM-VBL100 cells (Figure 6, left panel) and the 72-hour treatment with the antisense PONs virtually abrogated the
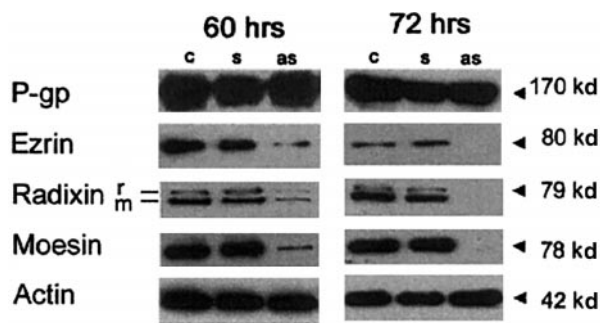
Figure 6. Effects of antisense PONs on ERM expression. Western blotting on membrane/cytoskeleton fraction of sense (s) or antisense (as) PON-treated or -untreated (c) CEM-VBL100 cells after a 60-hour (left panel) or a 72-hour (right panel) treatment. In both panels, 1 of 5 representative experiments is shown. Actin levels in the relative lysates are shown.

expression of ERM proteins (Figure 6, right panel), whereas both the 60-hour and the 72-hour treatments did not affect P-gp expression, as assessed by Western blot analysis (Figure 6, left and right panels). However, the 72-hour treatment reduced the viability of CEM-VBL100 cells (up to 10% of dead cells). For this reason, we used the 60-hour treatment approach to perform experiments aimed at evaluating the effects of antisense PON pretreatment on P-gp function. The effect of the treatment with the antisense PONs on CEM-VBL100 cells was tested using different approaches: (1) cell susceptibility to the cytotoxic effect of VBL, (2) intracellular retention of VBL-bodipy, (3) expression and cellular localization of P-gp, and (4) P-gp association with actin. The treatment of multidrug-resistant CEM-VBL100 cells with VBL was almost ineffective, whereas it induced a dramatic effect on the CCRF-CEM parental cell line (up to 70% cell death), as assessed by the live/dead viability/cytotoxicity test (Figure 7A). The ERM antisense PON pretreatment recruited VBL susceptibility (VBL-induced cell death) in CEM-VBL100 cells at levels comparable to
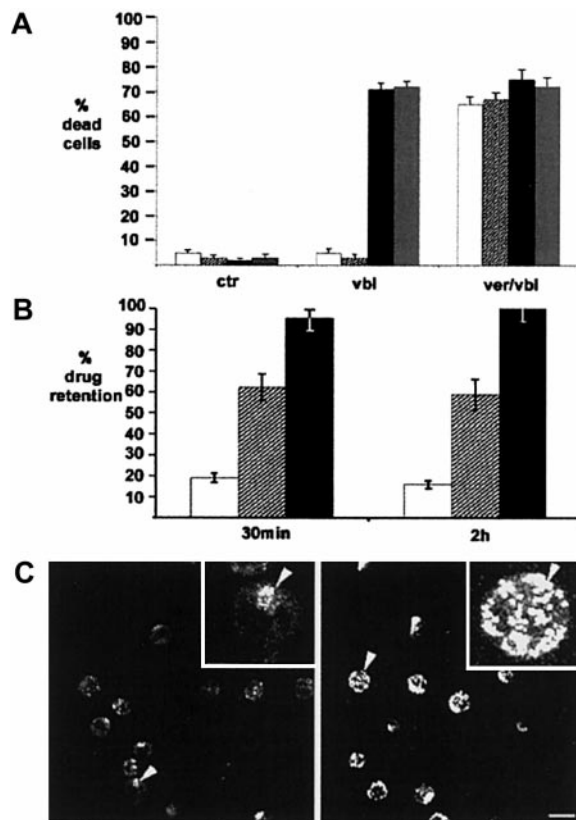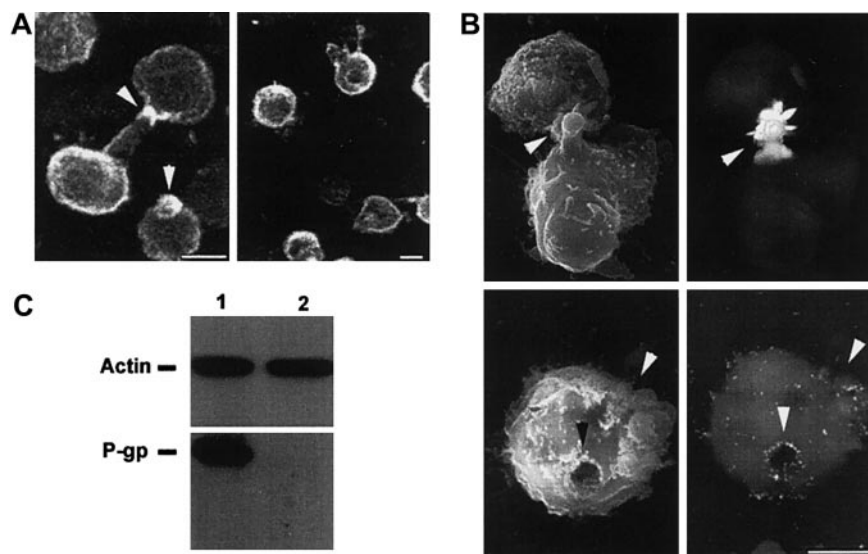

Figure 7. Effects of antisense PONs on P-gp activity. (A) The percentage of dead CEM-VBL100 cells untreated (□) or pretreated with sense (▨) or antisense (■) PONs, or parental CCRF-CEM cells (▤), and then treated with vinblastine (vbl), verapamil plus vinblastine (ver/vbl), or nothing (ctr), using the live/dead viability/cytotoxicity test (Molecular Probes). Histograms represent mean ± SD of 5 different experiments. In antisense-treated cells only, VBL susceptibility was significantly restored, at levels comparable to those in the parental CCRF-CEM line. (B) Flow cytometric analysis of percentage of drug retention in untreated (□) or antisense PON–treated (▨) CEM-VBL100 cells. Cells were incubated with VBL-bodipy (see "Materials and methods"), washed, and allowed to recover in fresh medium for the indicated times. As a positive control for P-gp activity inhibition, untreated CEM-VBL100 cells were incubated with VPL during the efflux time (■). The percentage of drug retention was calculated as the ratio between the MFC of each sample at the end of the efflux time and the MFC detected at the end of drug treatment, times 100. (C) Confocal microscopy analysis of VBL-bodipy retention in ERM sense (left panel) and antisense (right panel) PON-treated CEM-VBL100 cells in 1 of 5 representative experiments. The insets show magnifications of the cells pointed by the arrowheads, further illustrating the differences in the drug distribution between ERM sense and antisense treatments. Bar = 10 μm.

those in the parental CCRF-CEM cells (Figure 7A). Thus, we evaluated the drug retention in ERM antisense PON–treated cells as compared with untreated controls. The results showed that PON pretreatment induced a marked reduction of the P-gp–mediated efflux of VBL-bodipy from CEM-VBL100 cells, resulting in a 2- to 3-fold increase in drug retention as compared with untreated controls, as assessed by fluorescence-activated cell sorting analysis (Figure 7B). Moreover, LSCM analysis showed a clear increase in the retention as well as in the intracellular compartmentalization of the drug in the antisense PON–treated as compared with the sense PON–treated cells (Figure 7C). Untreated controls did not show any difference as compared with the sense PON–pretreated cells (not shown). These data are highly consistent with a marked variation in the P-gp distribution pattern in antisense PON–treated cells (Figure 8A,B). In fact, in antisense PON–treated cells, the P-gp staining appeared unpolarized and localized all around the cell, as assessed by both LSCM (Figure 8A, right panel) and immuno-SEM analysis (Figure 8B, lower panels), in comparison with the sense-PON–treated cells (Figure 8A, left panel and Figure 8B, upper panels, respectively) and untreated cells (not shown). These data are consistent with the coimmunoprecipitation experiments performed on lysates from antisense PON–treated cells. In fact, after the ERM antisense PON treatment, P-gp was no longer detectable in the actin immunoprecipitates (Figure 8C, low right lane), strongly suggesting that ERM had a key role in the association between P-gp and actin.

Discussion

To date, little attention has been directed toward the relation between P-gp expression and the actin microfilament system and the possible importance of the actin–P-gp interaction in the development of multidrug resistance at the cellular level. However, a few reports have indirectly suggested the involvement of this interaction in multidrug resistance.[40-42] In fact, it has been shown that actin-perturbing agents, such as cytochalasin, enhance the intracellular accumulation of drugs in leukemia cells.[43] More recently, it has been reported that MDR osteosarcoma cells exhibit a marked increase in actin stress-fiber organization. This finding was consistent with the increase in the drug's intracellular accumulation and cytotoxic effect through disruption of the stress-fiber network induced by actin perturbation.[14] These studies suggested that the organization of cellular actin associated with differentiation may be involved in the expression of P-gp function and in the development of multidrug resistance. There is growing evidence that the actin-filament association with a variety of cellular proteins is mediated by a class of highly specialized proteins—ezrin, radixin, and moesin—which cross-link actin filaments with the plasma membrane and drive the polarization of a cell.[19-22] In fact, various cellular functions, such as the formation of microvilli, cell–cell adhesion, maintenance of cell shape, cell motility and apoptosis, as well as membrane trafficking and signaling pathways, depend on membrane–cytoskeleton interactions.[22-31] In particular, it has been demonstrated that ion pumps, together with other membrane proteins, are mostly localized in well-established polarized sites of epithelial cells.[14,15] The polarization of these pumps is mediated by changes in the distribution and composition of the cytoskeleton,[14] as well as by the direct or indirect association of the pump-associated proteins with the actin cytoskeleton through the ERM proteins.[31] Notably, the specific alteration of actin–membrane interactions profoundly affects cell polarity and is associated with some diseases related to aberrant function of ion pumps.[44] These data made highly conceivable a possible linkage of P-gp with the actin cytoskeleton as a key mechanism in the development of the P-gp–mediated multidrug resistance. In a previous paper, we showed that treatment with IFN-γ induced in human monocyte-derived macrophages the translocation of P-gp to the plasma

Figure 8. Effects of antisense PONs on P-gp localization and actin association on CEM-VBL100 cells. (A) Immunofluorescence analysis of P-gp cellular distribution in ERM sense (left panel) and antisense (right panel) PON-treated CEM-VBL100 cells. Arrows (left panel) point to the polarized distribution of P-gp in sense PON–treated cells; in contrast, antisense PON–treated cells (right panel) did not show any feature of polarization, together with an altered P-gp distribution on the cell surface. Bar = 5 μm. (B) Immuno-SEM analysis of P-gp distribution in ERM sense (upper panels) and antisense (lower panels) PON-treated CEM-VBL100 cells. The polarized morphology of sense PON–treated CEM-VBL100 cells (arrows, upper left panel) was completely lost after antisense PON treatment (arrows, lower left panel). Consistently, P-gp distribution, highly polarized on uropoidal formations (arrows, upper right panel), was clearly altered and unpolarized in antisense PON–treated cells (arrows, lower right panel). No appreciable labeling was detected in control conjugate samples incubated with irrelevant mAb. Bar = 5 μm. In both (A) and (B), 1 of 5 representative experiments is shown. (C) Coimmunoprecipitation analysis of CEM-VBL100 cells pretreated with sense (1) or antisense (2) ERM PONs. Actin immunoprecipitates were separated by SDS-PAGE in nonreducing (upper panel) or reducing (lower panel) conditions (see "Materials and methods") and blotted with anti-actin or anti–P-gp mAb, respectively.

membrane, where it polarized and colocalized with ezrin.[11] This suggested both a role of P-gp–ERM–actin interaction in the physiologic function of a cell and the implication of this interaction in the development of multidrug resistance. The results of our present investigation clearly show that in a P-gp–expressing, multidrug-resistant human lymphoid T-cell line, P-gp polarized, colocalized, and coimmunoprecipitated with ERM proteins and actin. As a direct consequence of this interaction, P-gp clearly polarizes on cellular uropods. These findings are highly consistent with data of other authors independently showing the localization of ERM and actin[45] and P-gp[46,47] in well-defined membrane structures, such as caveolae or microdomains. This in turn may suggest that P-gp–ERM–actin interaction has a key role in localizing P-gp in well-defined membrane sites. The polarization of a protein on cellular cues or uropods has been related to a sort of economy of the cell.[21,22] On the basis of this hypothesis, a cell, to develop a given function, concentrates membrane molecules in defined sites instead of increasing protein synthesis. These sites correspond to constitutively polarized points in immobile cells, such as epithelial cells, and uropods in trafficking cells, such as lymphocytes and monocytes. In these cells, the uropods are the most probable contact sites with either other cells or extracellular matrix components.[21,22] Our results and previous reports on epithelial cells[48-50] strongly suggest that P-gp needs to be polarized

to fully exert its function. Consistent with this hypothesis, we showed that treatment with ERM antisense oligonucleotides recruited the sensibility of a human lymphoblastoid cell line, CEM-VBL100 cells, to the toxic effect of drugs, consistent with the inhibition of the P-gp–mediated pump, the intracellular retention of the drugs, and the unpolarized redistribution of P-gp on the cell surface. Finally, the ERM antisense oligonucleotide treatment virtually abrogated the P-gp linkage to actin, further suggesting that ERM proteins have a key role in the actin–P-gp association and, as a direct consequence, in the P-gp–mediated function. This set of results strongly suggests the following: (1) The polarized state is key for P-gp–mediated function, particularly in rendering a cell of lymphoid origin resistant to drug treatment; and (2) the association of P-gp with actin through the ERM proteins is crucial for the establishment and maintenance of P-gp polarization and, as a direct consequence, for the development of multidrug resistance.

Together, our data define for the first time a clear association between P-gp and the actin cytoskeleton through ERM proteins and a dramatic inhibition of the P-gp–mediated multidrug resistance after specific inhibition of ERM synthesis. Research on new molecules or gene-therapy strategies aimed at selectively modulating membrane–cytoskeleton associations and the P-gp–mediated multidrug resistance, to improve the efficacy of both antitumor and antiviral treatments, may stem from the results of this study.

References

1. Juranka PF, Zastawny RL, Ling V. P-glycoprotein: multidrug-resistance and a superfamily of membrane-associated transport proteins. FASEB J. 1989;3:2583-2592.

2. Nielsen D, Skovsgaard T. P-glycoprotein as multidrug transporter: a critical review of current multidrug resistant cell lines. Biochim Biophys Acta. 1992;1139:169-183.

3. Ueda K, Okamura N, Hirai M, et al. Human P-glycoprotein transports cortisol, aldosterone, and dexamethasone, but not progesterone. J Biol Chem. 1992;267:24248-24252.

4. Antonelli G, Turriziani O, Cianfriglia M, et al. Resistance of HIV-1 to AZT might also involve the cellular expression of multidrug resistance P-glycoprotein. AIDS Res Hum Retroviruses. 1992;8:1839-1844.

5. Tsuruo T, Iida H, Nojiri M, Tsukagoshi S, Sakurai Y. Circumvention of vincristine and adriamycin resistance in vitro and in vivo by calcium influx blockers. Cancer Res. 1983;43:2905-2910.

6. Tsuruo T, Iida H, Tsukagoshi S, Sakurai Y. Potentiation of vincristine and adriamycin effects in human hemopoietic tumor cell lines by calcium antagonists and calmodulin inhibitors. Cancer Res. 1983;43:2267-2272.

7. Sarkadi B, Muller M, Homolya L, et al. Interaction of bioactive hydrophobic peptides with the human multidrug transporter. FASEB J. 1994;8:766-770.

8. Sharom FJ, DiDiodato G, Yu X, Ashbourne KJ. Interaction of the P-glycoprotein multidrug transporter with peptides and ionophores. J Biol Chem. 1995;270:10334-10341.

9. Gupta S, Gollapudi S. P-glycoprotein (MDR-1 gene product) in cells of the immune system: its possible physiologic role and alteration in ageing and human immunodeficiency virus-1 (HIV-1) infection. J Clin Invest. 1993;13:289-301.

10. Ludescher C, Pall G, Irschick EU, Gasti G. Differential activity of P-glycoprotein in normal blood lymphocyte subset. Br J Haematol. 1998;101:722-727.

11. Puddu P, Fais S, Luciani F, et al. Interferon-γ upregulates expression and activity of P-glycoprotein in human peripheral blood monocyte-derived macrophages. Lab Invest. 1999;79:1299-1309.

12. Lee CG, Gottesman MM, Cardarelli CO, et al. HIV-1 protease inhibitors are substrates for the MDR1 multidrug transporter. Biochemistry. 1998;37:3594-3601.

13. Cianfriglia M, Cenciarelli C, Tombesi M, et al. Murine monoclonal antibody recognizing a 90-kDa cell-surface determinant selectively lost by multidrug-resistant variants of CEM cells. Int J Cancer. 1990;45:95-103.

14. Takeshita H, Kusuzaki K, Ashihara T, Gebhardt MC, Mankin HJ, Hirasawa Y. Actin organization associated with the expression of multidrug resistant phenotype in osteosarcoma cells and the effect of actin depolymerization on drug resistance. Cancer Lett. 1998;126:75-81.

15. Bichat F, Mouawad R, Solis-Recendez G, Khayat D, Bastian G. Cytoskeleton alteration in MCF7R cells, a multidrug resistant human breast cancer cell line. Anticancer Res. 1997;17:3393-3402.

16. Bretscher A. Regulation of cortical structure by the ezrin-radixin-moesin protein family. Curr Opin Cell Biol. 1999;11:109-116.

17. Mangeat P, Roy C, Martin M. ERM proteins in cell adhesion and membrane dynamics. Trends Cell Biol. 1999;9:187-192.

18. Drubin DG, Nelson WJ. Origins of cell polarity. Cell. 1996;84:335-344.

19. Fais S, Luciani F, Logozzi M, Parlato S, Lozupone F. Linkage between cell-membrane proteins and actin-based cytoskeleton: the cytoskeleton-driven cellular functions. Histol Histopathol. 2000;15:539-549.

20. Luna EJ, Hitt AL. Cytoskeleton-plasma membrane interactions. Science. 1992;258:955-963.

21. Nelson WJ. Regulation of cell surface polarity from bacteria to mammals. Science. 1992;258:948-955.

22. Kusumi A, Sako Y. Cell surface organization by the membrane skeleton. Curr Opin Cell Biol. 1996;8:566-574.

23. Dransfield DT, Bradford AJ, Smith J, et al. Ezrin is a cyclic AMP-dependent protein kinase anchoring protein. EMBO J. 1997;16:35-43.

24. Tsukita S, Yonemura S, Tsukita S. ERM (ezrin/radixin/moesin) family: from cytoskeleton to signal transduction. Curr Opin Cell Biol. 1997;9:70-75.

25. Defacque H, Egeberg M, Habermann A, et al. Involvement of ezrin/moesin in de novo actin assembly on phagosomal membranes. EMBO J. 2000;19:199-212.

26. Tsukita S, Oishi S, Sato N, Sagara J, Kawaki A, Tsukita S. ERM family proteins as molecular linkers between the cell surface glycoprotein CD44 and actin-based cytoskeleton. J Cell Biol. 1994;126:391-401.

27. Parlato S, Giammarioli AM, Logozzi M, et al. CD95 (APO-1/Fas) linkage to the actin cytoskeleton through ezrin in human T-lymphocytes: a novel regulatory mechanism of the CD95 apoptotic pathway. EMBO J. 2000;19:5123-5134.

28. del Pozo MA, Sanchez-Mateos P, Sanchez-Madrid F. Cellular polarization induced by chemokines: a mechanism for leukocyte recruitment? Immunol Today. 1996;17:127-131.

29. Rizzolo LJ. Polarization of the Na⁺, K⁺-ATPase in epithelia derived from the neuroepithelium. Int Rev Cytol. 1999;185:195-235.

30. Rodriguez-Boulan E, Nelson WJ. Morphogenesis of the polarized epithelial cell phenotype. Science. 1989;245:718-725.

31. Moyer BD, Duhaime M, Shaw C, et al. The PDZ-interacting domain of cystic fibrosis transmembrane conductance regulator is required for functional expression in the apical plasma membrane. J Biol Chem. 2000;275:27069-27074.

32. Cianfriglia M, Willingham MC, Tombesi M, Scagliotti GV, Frasca G, Chersi A. P-glycoprotein epitope mapping. I. Identification of a linear human-specific epitope in the fourth loop of the P-glycoprotein extracellular domain by MM4.17 murine monoclonal antibody to human multidrug-resistant cells. Int J Cancer. 1994;56:153-160.

33. Fais S, Pallone F. Inability of normal human intestinal macrophages to form multinucleated giant cells in response to cytokines. Gut. 1995;37:798-801.

34. Noonan KE, Beck C, Holzmayer TA, et al. Quantitative analysis of MDR1 (multidrug resistance) gene expression in human tumors by polymerase chain reaction. Proc Natl Acad Sci U S A. 1990;87:7160-7164.

35. Di Marzio P, Puddu P, Conti L, Belardelli F, Gessani S. Interferon gamma upregulates its own gene expression in mouse peritoneal macrophages. J Exp Med. 1994;179:1731-1736.

36. Bukrinskaya A, Brichacek B, Mann A, Stevenson M. Establishment of a functional human immunodeficiency virus type 1 (HIV-1) reverse transcription complex involves the cytoskeleton. J Exp Med. 1998;188:2113-2125.

37. Laemmli UK. Cleavage of structural proteins during the assembly of the head of bacteriophage T4. Nature. 1970;227:680-685.

38. Lee CGL, Gottesmann MM. HIV-1 protease inhibitors and the MDR1 multidrug transporter. J Clin Invest. 1998;101:287-288.

39. Shcherbina A, Bretscher A, Kenney DM, Remold-O'Donnel E. Moesin, the major ERM protein of lymphocytes and platelets, differs from ezrin in its insensitivity to calpain. FEBS Lett. 1999;443:31-36.

40. Erokhina MV, Shtil AA, Shushanov SS, Sidorova TA, Stavrovskaja AA. Partial restoration of the actin cytoskeleton in transformed Syrian hamster fibroblasts selected for low levels of "typical" multidrug resistance. FEBS Lett. 1994;341:295-298.

41. Cauda R, Lucia MB, Ortona L, Rainaldi G, Donelli G, Malorni W. A new, striking morphological alteration of P-glycoprotein expression in NK cells from AIDS patients. Immunol Lett. 1998;60:19-21.

42. Capella LS, Alcantara JS, Moura-Neto V, Lopes AG, Capella MA. Vanadate is toxic to adherent-growing multidrug-resistant cells. Tumour Biol. 2000;21:54-62.

43. Tsuruo T, Iida H. Effects of cytochalasins and colchicine on the accumulation and retention of daunomycin and vincristine in drug resistant tumor cells. Biochem Pharmacol. 1986;35:1087-1090.

44. Wilson PD. Epithelial cell polarity and disease. Am J Physiol. 1997;272:F434–F442.

45. Michaely PA, Mineo C, Ying Y, Anderson RGW. Polarized distribution of endogenous Rac1 and RhoA at the cell surface. J Biol Chem. 1999;274:21430-21436.

46. Lavie Y, Fiucci G, Liscovitch M. Up-regulation of caveolae and caveolar constituents in multidrug-resistant cancer cells. J Biol Chem. 1998;273:32380-32383.

47. Demeule M, Jodoin J, Gingras D, Beliveau R. P-glycoprotein is localized in caveolae in resistant cells and in brain capillaries. FEBS Lett. 2000;466:219-224.

48. Hammerle SP, Rothen-Rutishauser B, Kramer SD, Gunthert M, Wunderli-Allenspach H. P-glycoprotein in cell cultures: a combined approach to study expression, localisation, and functionality in the confocal microscope. Eur J Pharm Sci. 2000;12:69-77.

49. Kim RB, Fromm MF, Wandel C, et al. The drug transporter P-glycoprotein limits oral absorption and brain entry of HIV-1 protease inhibitors. J Clin Invest. 1998;101:289-294.

50. Tatsuta T, Naito M, Oh-hara T, Sugawara I, Tsuruo T. Functional involvement of P-glycoprotein in blood-brain barrier. J Biol Chem. 1992;267:20383-20391.